Dartmouth College

Dartmouth Digital Commons

Open Dartmouth: Published works by Dartmouth faculty

Faculty Work

Orbital Period of the Low-Inclination SW Sextantis Star V442 Ophiuchi

D. W. Hoard
Cerro Tololo Inter-American Observatory

John R. Thorstensen
Dartmouth College

Paula Szkody
University of Washington

Follow this and additional works at: https://digitalcommons.dartmouth.edu/facoa

Part of the Stars, Interstellar Medium and the Galaxy Commons

ORBITAL PERIOD OF THE LOW-INCLINATION SW SEXTANTIS STAR V442 OPHIUCHI[1]

D. W. HOARD

Cerro Tololo Inter-American Observatory Casilla 603, La Serena, Chile; dhoard@noao.edu

JOHN R. THORSTENSEN

Department of Physics and Astronomy, Dartmouth College, 6127 Wilder Laboratory, Hanover, NH 03755-3528; thorstensen@dartmouth.edu

AND

PAULA SZKODY

Department of Astronomy, University of Washington Box 351580, Seattle WA 98195-1580; szkody@astro.washington.edu

Received 1999 November 22; accepted 2000 February 17

ABSTRACT

V442 Ophiuchi is a low-inclination (noneclipsing) nova-like cataclysmic variable. We have obtained medium resolution (1–3.5 Å), time-resolved optical spectroscopy of this interacting binary star spanning an interval of 4 yr, from 1995 August to 1999 June. Using an Hα radial velocity curve constructed from our combined spectroscopic data sets, we have determined that $P_{orb} = 0.1243$ days for V442 Oph, breaking the long-standing 1 day alias ambiguity in its orbital period. V442 Oph shares many of the characteristics of the group of cataclysmic variables known as the SW Sextantis stars. Its Doppler tomograms and orbital phase–dependent emission-line behavior, including the occurrence of a prominent transient absorption event, are consistent with those of other SW Sex stars. V442 Oph also displays single-peaked rather than double-peaked emission lines, strong He II λ4686 emission, and a phase offset of $+0.08$ between the Hα emission-line radial velocities and the phasing of He II. We discuss the role of V442 Oph as one of three known low-inclination examples of SW Sex stars. Like the other low-inclination SW Sex stars, LS Pegasi and V795 Herculis, the Balmer emission lines in V442 Oph have high velocity components that extend to $\approx \pm 1900$ km s^{-1} and follow an apparent S-wave pattern in the trailed spectrum. Finally, we compare two models for the SW Sex stars involving accretion stream overflow, in the context of a low-inclination system in which our line of sight likely extends over the entire face of the disk.

Subject headings: accretion, accretion disks — novae, cataclysmic variables — stars: individual (V795 Herculis, V442 Ophiuchi, LS Pegasi)

1. INTRODUCTION

V442 Ophiuchi was identified as a cataclysmic variable (CV) by Szkody & Wade (1980) based on its photometric and spectroscopic properties. They noted that He II λ4686 emission was comparable in strength to Hβ. A follow-up investigation by Szkody & Shafter (1983) utilized photometry and spectroscopy in the IR, optical, and UV. They measured an orbital period $P_{orb} = 0.1403$ days ($=7.13$ cycles day^{-1}) from Hα and He II λ4686 radial velocity curves and found a roughly sinusoidal variation in the J-band light curve consistent with this period (presumably caused by the changing visibility of the irradiation-heated inner face of the secondary star.) However, extensive time series optical photometry did not reveal any evidence of an eclipse, implying a system inclination $i \lesssim 65°$. Recently, J. Patterson (1998, private communication) has suggested an orbital period of $P_{orb} = 0.1243$ days ($=8.06$ cycles day^{-1}) based on an ≈ 0.02 mag modulation in an as yet unpublished light curve of V442 Oph. As the proposed periods are 1 day aliases of each other, our current investigation of V442 Oph was motivated in part by the need to measure unambiguously its orbital period.

A second motivating factor was the identification of V442 Oph as a member of the group of CVs known as the SW Sextantis stars. These are nova-like CVs sharing a number of observational characteristics (e.g., Hoard 1998;[2] Thorstensen et al. 1991, and reviewed by Warner 1995): (1) single-peaked emission lines (rather than the double-peaked lines expected from a rotating accretion disk); (2) strong He II λ4686 emission (comparable to Hβ); (3) phase offsets between the emission-line radial velocity curves and eclipse ephemerides (producing emission regions located at unusual positions in their Doppler tomograms); (4) Balmer and He I emission lines that are only shallowly eclipsed compared to the continuum (implying emission originating above the orbital plane); and (5) orbital phase–dependent transient absorption features that appear in the Balmer and He I emission line cores. The SW Sex stars are often, but not always, high-inclination eclipsing systems with 3 hr $\leq P_{orb} \leq 4$ hr. Two other noneclipsing CVs, LS Pegasi ($=$S193; Martínez-Pais, Rodríguez-Gil, & Casares 1999; Taylor, Thorstensen, & Patterson 1999) and V795 Herculis (Casares et al. 1996; Dickinson et al. 1997), have been proposed as examples of low-inclination SW Sex stars.[3] Hoard (1998; also see Hoard & Szkody 1999) suggested that V442 Oph is the third known low-inclination SW Sex star based on its single-peaked emission lines, strong He II emission, and a weak transient absorption feature observed in spectra from 1995. We confirm that conclusion here with an

---

[1] Based on data obtained using the 2.4 m Hiltner telescope of the Michigan-Dartmouth-M.I.T. Observatory and the Apache Point Observatory 3.5 m telescope, which is owned and operated by the Astrophysical Research Consortium.

[2] Available at http://www.ctio.noao.edu/~hoard/dissertation/diss.html.

[3] WX Arietis, which was originally proposed as the first low-inclination SW Sex star (Beuermann et al. 1992; Chen et al. 1993; Hellier, Ringwald, & Robinson 1994) has recently been shown to have shallow ($\Delta R \approx 0.15$ mag) eclipses and a likely inclination of $i \sim 72°$ (Rodríguez-Gil et al. 1999).

analysis of Doppler tomograms of V442 Oph constructed from spectra phased using our firmly determined orbital period.

2. OBSERVATIONS

In 1995 August and 1998 April, we obtained two sets of time-resolved, medium-resolution (1–2 Å) optical (4300–5100 Å, 5800–6800 Å) spectra of V442 Oph using the Double Imaging Spectrograph on the Apache Point Observatory (APO) 3.5 m telescope (Gillespie, Loewenstein, & York 1995; details of the instrument setup can be found in Hoard 1998). Exposure times were 600 s in 1995 and 150 or 300 s in 1998. A total of 13 spectra were acquired on 1995 August 28–29 UT, and 71 on 1998 April 8–10 UT.

The initial analysis of the APO data (Hoard & Szkody 1999) left the orbital frequency ambiguous by ±1 cycle day^{-1} because on the dates of observation, the transits of the source were too far from local midnight for us to obtain sufficient coverage modulo 1 day. To resolve the ambiguity we obtained additional medium-resolution (3.5 Å) optical (4200–7600 Å) spectra of V442 Oph in 1999 June with the 2.4 m Hiltner telescope at the Michigan-Dartmouth-MIT (MDM) Observatory. The instrumentation and procedures were essentially the same as those described by Thorstensen, Taylor, & Kemp (1998). We obtained a total of 14 spectra in 13 short visits to the source on 1999 June 4 and 9–10 UT; exposure times were 180–300 s. To provide maximum leverage in resolving the orbital period ambiguity, the observations were arranged to span a large hour angle range of 6^{h}35.

Figure 1 shows representative spectra from each observing run. Although the instrumental response was successfully removed from the spectra via observations of spectrophotometric standard stars (Massey et al. 1988)
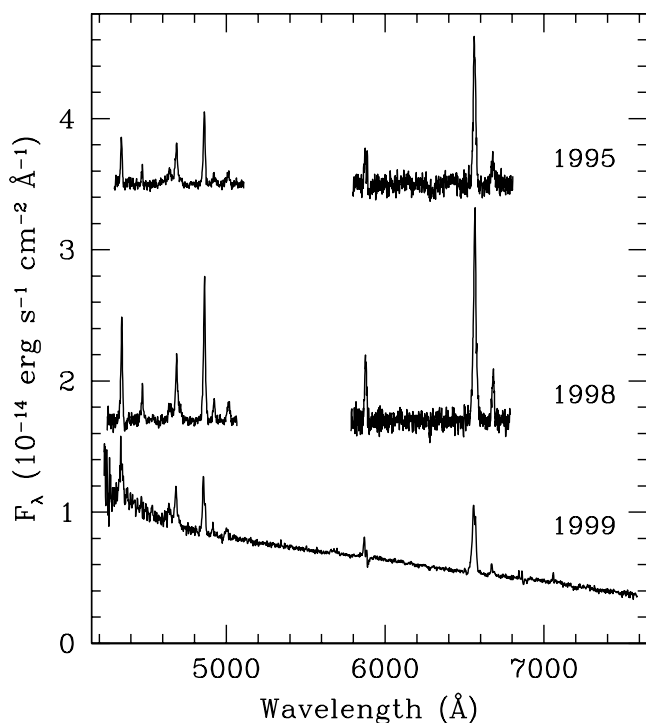

FIG. 1.—Representative spectra of V442 Oph from each observing run. The flux scale is accurate for the 1999 spectrum; the 1995 and 1998 spectra have been normalized to a constant continuum of 1.0 and shifted by arbitrary amounts for clarity.
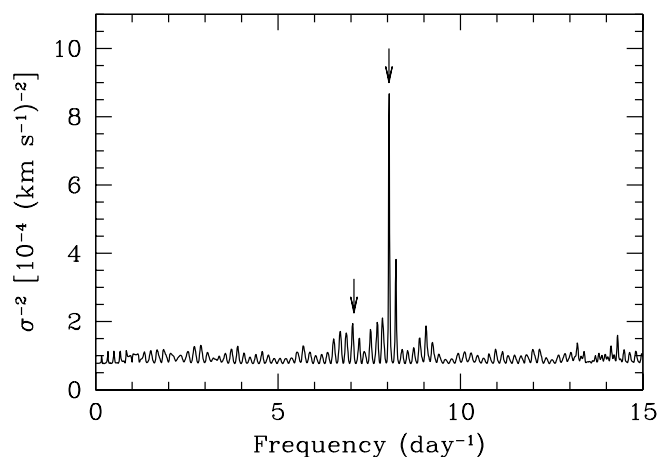

FIG. 2.—Periodogram of the Hα radial velocities from the MDM spectra. Arrows mark our adopted orbital period (prominent peak just above 8 cycles day^{-1}) and the 1 day alias (small peak just above 7 cycles day^{-1}).

obtained during each observing run, slit losses in the APO data are likely to have rendered their absolute flux level calibration unreliable.

3. ORBITAL PERIOD

We measured radial velocities in the 1999 June MDM spectra using a double-Gaussian convolution method (Schneider & Young 1980) with individual Gaussians of 10 Å FWHM separated by 44 Å center to center. This essentially gave velocities of the line wings. Figure 2 shows a periodogram of the MDM velocities, rendered as the inverse square of the rms residual to the best sinusoidal fit at each trial frequency (Thorstensen et al. 1996). Thanks to the large hour angle range of the MDM spectra, one frequency stands out strongly among the various possibilities. A sinusoidal fit of the form

$$v(t) = \gamma + K \sin\left[2\pi(t - T_0)/P_{\rm orb}\right]$$

yielded the parameters given for the MDM data in Table 1.

Figure 3 shows the MDM velocities (*large filled circles*) folded on the best-fit orbital period, $P_{\rm orb} = 0.12435(7)$ days (*solid curve*). Because these Hα velocities (and those
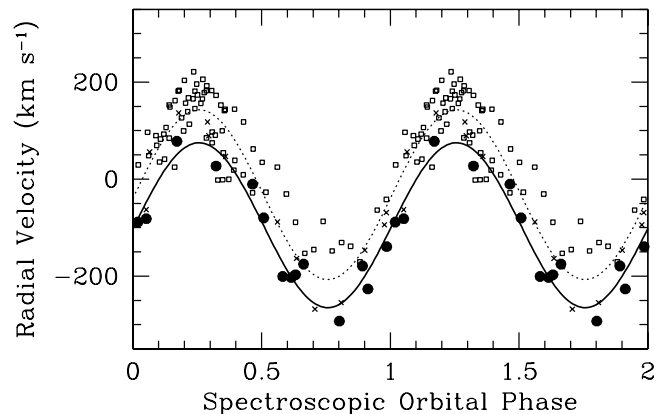

FIG. 3.—Hα radial velocities from the MDM data (*large filled circles*) and APO data (small squares for 1998 April; small crosses for 1995 August). The solid curve shows the best sinusoidal fit to the MDM data, while the dotted curve shows the best fit to the combined data. All data are plotted twice for clarity.

TABLE 1

LOG OF OBSERVATIONS AND FITS TO Hα RADIAL VELOCITIES

UT Date	Site	N	T_0[a]	P (days)	K (km s^{-1})	γ (km s^{-1})	σ (km s^{-1})
1995 Aug 28–29	APO	13	49957.7161(19)	0.1250(4)	180(17)	−56(12)	33
1998 Apr 8–10	APO	71	50912.9475(14)	0.1233(3)	149(9)	7(6)	45
1999 Jun 4, 9–10......	MDM	14	51338.6563(17)	0.12435(7)	170(19)	−95(11)	34
Combined	...	98	50911.8281(15)	0.1243302(4)[b]	175(8)	−32(3)	55

[a] Apparent emission line inferior conjunction (blue-to-red crossing), HJD −2400000.
[b] Precise period is based on an arbitrary choice of cycle count— see text.

obtained from the other data sets) are unlikely to trace the motion of either star in this system, we caution against using K or γ to estimate component masses and other parameters of the system geometry. We note that an orbital period of ≈0.124 days places V442 Oph at the upper end of the so-called CV period gap (e.g., Shafter 1992).

In order to verify that the 1 day alias ambiguity was really resolved, we used the Monte Carlo test described by Thorstensen & Freed (1985) to test our best period against the alternative at 0.1412 days. The correctness likelihood for our period was indistinguishable from unity in a 1000 trial simulation. The strongest secondary peak in our periodogram is actually at 0.1215 days (= 8.23 cycles day^{-1}; the second tallest peak in Fig. 2, just to the high-frequency side of the primary peak) and arises from a 5 day gap in the spectroscopic observations. A conservative Monte Carlo test yields a correctness likelihood near 1% for this period, so it can also be disregarded.

We measured Hα radial velocities from the APO spectra in the same manner as for the MDM data. The best-fit period from the 1998 April data differs from the 1999 June period by 3.4 of their mutual standard deviation, and the γ-velocity of the former is significantly higher (see Table 1). However, the 1998 April data suffered from a particularly uneven phase distribution, so the formal errors on the fit parameters may be underestimated. Combining all the data together, and assuming phase coherence, yields a modest number of possible periods (each uncertain by about $\pm 4 \times 10^{-7}$ days) that are consistent with the 1999 June period at ±3 standard deviations. The APO Hα radial velocity measurements are shown (as small points) in Figure 3, overlaid with the sine function that best fits the combined (APO + MDM) data (dotted curve). We do not advocate the general use of T_0 and P_{orb} obtained from the combined data to provide a rigorous long-term ephemeris for V442 Oph because we cannot guarantee phase coherence over the 4 yr span of the three data sets.

4. DOPPLER TOMOGRAPHY

We constructed Doppler tomograms from the 1998 April 9 UT spectra (our best sampled data set) using the Fourier-filtered back-projection algorithm (Horne 1991; Kaitchuck et al. 1994 and references therein). Tomograms for Hα, Hβ, He II λ4686, and He I λ4471 are shown in Figure 4. The spectra were phased according to the best-fit sine function of the combined Hα radial velocity data set. Since V442 Oph does not eclipse, the phase zero point was set by determining the arbitrary phase offset that caused the He II emission to be situated symmetrically on the −V_y-axis of the tomogram, at the expected location of the white dwarf (WD) primary star. The phase offset value was Δφ = +0.58 relative to φ = 0.0 at the inferior conjunction (blue-to-red

crossing) of the Hα emission line source (as it is defined in § 3), or Δφ = +0.08 relative to the more common convention of φ = 0.0 at the superior conjunction (red-to-blue crossing) of the emission line source (which coincides with eclipse of the WD in high-inclination systems that have emission originating symmetrically around the WD). Henceforth, we refer to all orbital phases using the latter convention. The He II tomogram of V442 Oph implies an observed orbital velocity of $K_{wd} \sin i \approx 100$ km s^{-1} for the WD. The phase-corrected Hα and Hβ tomograms (as well as that of He II) are also very similar to those found for high-inclination examples of SW Sex stars (e.g., BH Lyncis, Hoard & Szkody 1997; PX Andromedae, Hellier & Robinson 1994). In addition, a phase offset of ~ +0.1 between the Balmer and He II emission-line velocities (demonstrated here for V442 Oph by the +0.08 offset between the Hα velocity curve and the He II tomogram) is a distinguishing characteristic of the SW Sex stars (e.g., Hoard 1998).

We also constructed Hα tomograms (not shown) from our other sets of spectra using the same phasing and phase offset as for the 1998 April 9 UT tomograms. Although they are of lower quality owing to sparser orbital phase coverage, they are very similar to the 1998 April Hα tomogram, showing an apparent ringlike structure and enhanced emission in the $(-V_x, -V_y)$ quadrant.

The presence of prominent emission in the $(+V_x, +V_y)$ quadrant in the He I λ4471 tomogram from 1998 April 9 UT is unusual, even for an SW Sex star, and defies a simple physical explanation. The He I λ4471 line is too weak and/or sparsely phase-sampled in the other data sets to provide useful tomograms, with the exception of the 1998 April 10 UT data. The He I tomogram constructed from these spectra is shown in Figure 5. It shows much the same structure as seen in the 1998 April 9 UT tomogram. Tomograms (not shown) of other He I lines (e.g. λλ4921, 5015) in V442 Oph from the 1998 April 9 UT spectra are substantially similar to that of the λ4471 line.

The Balmer and, especially, He I tomograms are also consistent with the presence of an absorbing source that is apparently at rest (or at least with $v \sin i \approx 0$) relative to the system's orbital motion. This accounts for the deep (below the continuum level) absorption at the origin of the He I tomogram and the less prominent absorption at the centers of the Balmer tomograms. (Doppler-shifting of emission from opposite edges of the disk in high-inclination CVs is typically expected to produce double-peaked emission lines that correspond to ring-shaped tomograms. However, in V442 Oph the ringlike appearance of the Balmer tomograms is caused by the low-velocity absorption—the emission lines are single-peaked away from the absorption event.) At the same time that the absorbing source is constrained to low velocity, it is also confined to a phase range
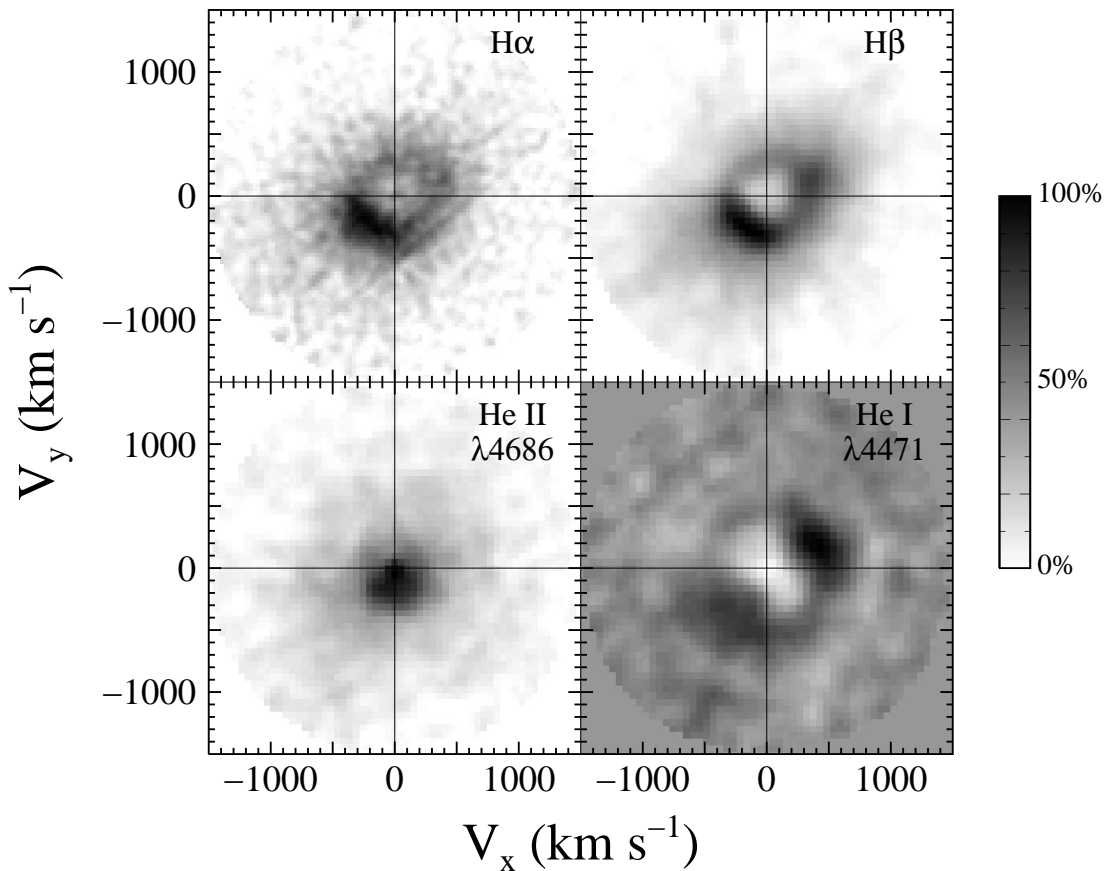
FIG. 4.—Doppler tomograms of V442 Oph emission lines. The intensity scale extends from the spectral continuum (0%) to the emission peak (100%), except in the He I tomogram, where it starts at the deepest absorption below the continuum (0%) and extends through the continuum ($\approx 45\%$) and emission peak (100%).

of $\phi \approx 0.2$–0.5 (relative to the orientation of the He II tomogram; also see § 5.1). This phase range for the absorption occurs somewhat earlier than the $\phi \approx 0.4$–0.7 seen in three other SW Sex stars by Szkody & Piché (1990), but Thorstensen et al. (1991) found a phase range of $\phi \approx 0.16$–0.66 (deepest at $\phi \approx 0.25$–0.50) in somewhat higher S/N
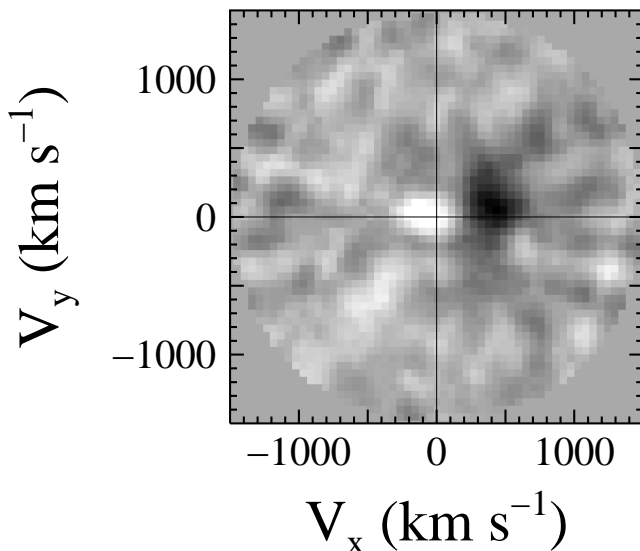
spectra of the SW Sex star PX And. A physical explanation for the transient absorption in V442 Oph is not immediately obvious. For example, the wind + stream-overflow model for the SW Sex stars proposed by Hellier (1999) predicts absorption in the ($-V_x$, $+V_y$) quadrant (which may or may not be present in our tomograms but is certainly not the most prominent absorbing region) and *emission* from a wind at low velocities near the origin of the tomogram.

We note in closing this section that the interpretation of our V442 Oph tomograms (despite their agreement in overall appearance with those of other SW Sex stars) must be considered at least somewhat suspect since the data used to construct them violate one of the fundamental assumptions of tomography; namely, that the emitting regions be equally visible at all orbital phases. However, this is almost certainly also true for the analysis of *all* other SW Sex star tomograms, so at least we are on an equal footing.

5. SPECTROSCOPIC CHARACTERISTICS

5.1. Transient Absorption

Perhaps the most unusual feature of the SW Sex stars is the presence of orbital phase–dependent transient absorption features in the Balmer and He I emission-line cores. Hoard (1998) reported a transient absorption feature that was weakly present in the Balmer lines of one of our time-resolved spectra of V442 Oph from 1995. This was reminiscent of the SW Sex star behavior but not strong enough to be conclusive. However, the emission lines of V442 Oph

FIG. 5.—He I $\lambda 4471$ tomogram of V442 Oph from 1998 April 10 UT

underwent a very pronounced transient absorption event in the 1998 April 9 UT data set—see Figure 6. This is reflected in the unusual tomogram of He I $\lambda4471$ (see Fig. 4), which shows a strong absorbing region near the velocity origin as well as weaker absorption regions in the $(-V_x, +V_y)$ and $(+V_x, -V_y)$ quadrants. The Balmer and He I, but not He II, lines are affected by the transient absorption, as is typical for the SW Sex stars. The duration of the event is ≈ 0.03 days, roughly 25% of the total orbital period. This is comparable to durations of $\approx 30\%$ of P_{orb} observed in DW Ursae Majoris, V1315 Aquilae, and SW Sex itself (Szkody & Piché 1990).

At its deepest, the absorption reaches well below the continuum in the He I lines. The deepest absorption occurs when the host emission-line core has maximum blueshift (i.e., at orbital phase $\phi \approx 0.5$ in most SW Sex stars; e.g. BH Lyn, Hoard & Szkody 1997). At onset, the absorption is redshifted relative to the host line rest wavelength; at its deepest, the absorption passes through λ_{rest}. It returns to a positive velocity shift as it vanishes. This is the same pattern followed by the $\phi \approx 0.5$ absorption in other SW Sex stars (e.g. DW UMa, V1315 Aql, SW Sex, Szkody & Piché 1990; PX And, Thorstensen et al. 1991). Although one or more spectra in all of our other data sets exhibit the presence of a central absorption feature in the Balmer and He I lines, no other such time-resolved absorption *event* is contained in

our data. However, it could have simply gone undetected owing to the poorer orbital phase coverage and sampling in the other data sets. Interestingly, Szkody (1991) reports the presence of highly variable absorption features in the emission lines of LS Peg (one of the other low-inclination SW Sex stars) that can change from strong (below the continuum) to nonexistent on timescales as short as 10 minutes or less.

5.2. High-Velocity Emission

A high-velocity emission component is present in the Hα line of V442 Oph (see Fig. 7), extending to almost -2000 km s^{-1} at $\phi \approx 0.4$ and to $\approx +1800$ km s^{-1} at $\phi \approx 0.9$. A similar, but weaker, high-velocity component with the same relative phasing is also seen in Hβ (see Fig. 8), extending to
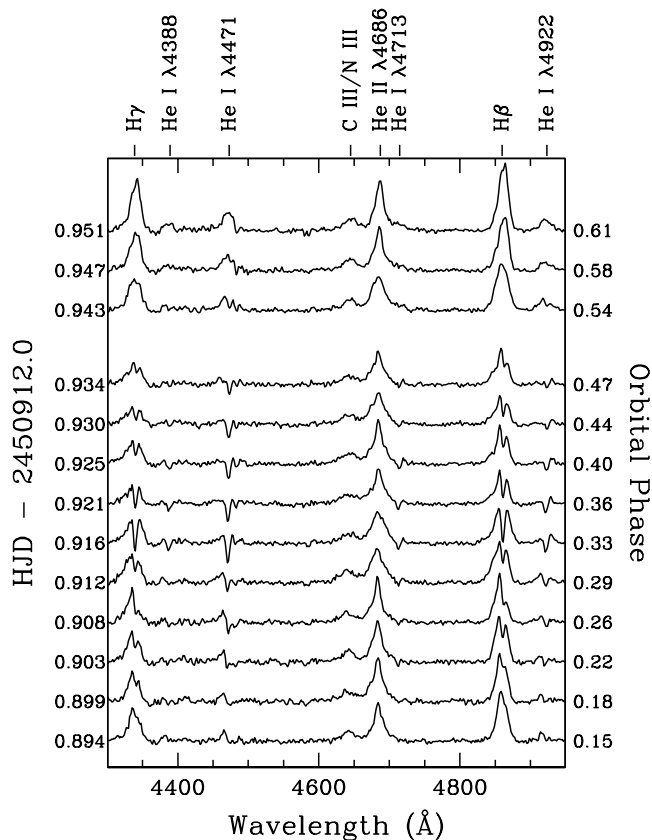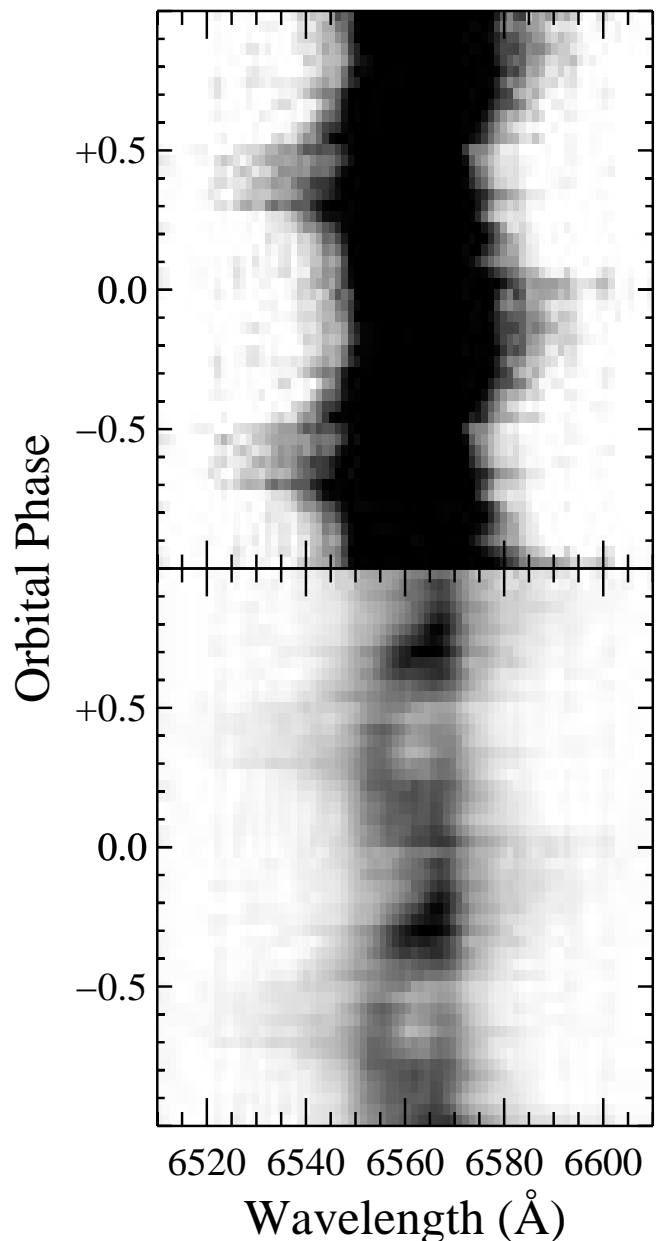

FIG. 6.—A subset of the spectra from 1998 April 9 UT. The vertical axis on the left shows the midpoint time of each spectrum, while the vertical axis on the right shows the spectroscopic phase corrected from the He II tomogram (see text) to approximate the "normal" orbital phasing convention (i.e., superior conjunction of the WD at phase 0.0). Note the deep transient absorption feature in the Balmer and especially He I lines, and the strong, single-peaked He II line.

FIG. 7.—Trailed spectrum of the Hα emission line in V442 Oph on 1998 April 9 UT. The bottom panel shows the full intensity range of the data, while the line core in the upper panel has been saturated to highlight the weaker high-velocity emission component.
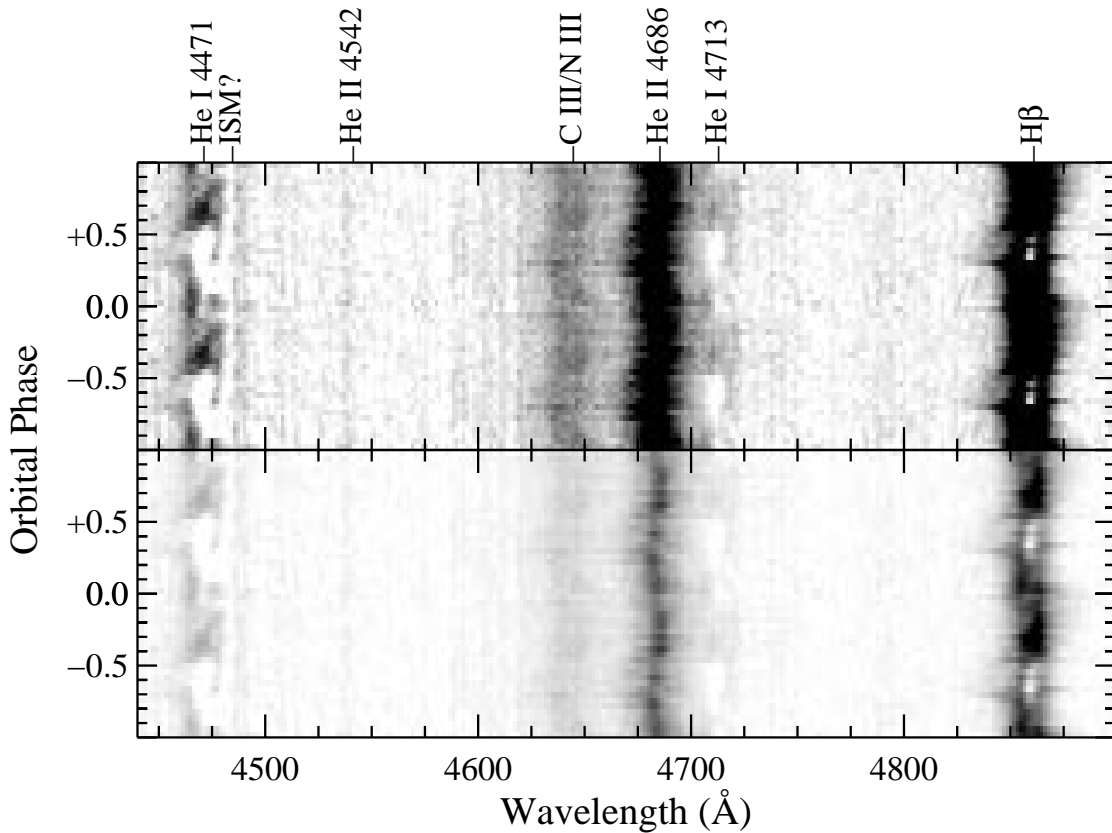
Fig. 8.—As in Fig. 7, but for the blue spectrum of V442 Oph. The narrow feature near He I λ4471 appears to be an interstellar medium absorption line (possibly Mg II λ4481) as it displays no velocity shifts.

≈ -1900 km s^{-1} and $\approx +1500$ km s^{-1}. Balmer emission extending to a large velocity shift from the line core is a distinguishing feature of the SW Sex stars but typically has smaller maximum extent in the high-inclination systems (e.g., ± 800–1000 km s^{-1} in PX And, V1315 Aql, and BH Lyn; Hellier & Robinson 1994, Hellier 1996, and Hoard & Szkody 1997, respectively). The other low-inclination SW Sex stars, V795 Her and LS Peg, also display a high-velocity emission component in their Hα and other Balmer lines with similar phasing and maximum velocity limits to that seen in V442 Oph. The fact that a similar high-velocity emission component has been observed in all three low-inclination SW Sex stars suggests that this feature may originate in the inner disk such that it can be seen only when the system is oriented to provide a line of sight to the inner disk. Taylor et al. (1999) demonstrated that the high-velocity component in LS Peg maps to a broad, diffuse emission region in the $(-V_x, -V_y)$ quadrant of the Doppler tomogram. This can also be seen in our Balmer tomograms of V442 Oph (see Fig. 4). This emission region is identified with the reimpact with the disk of an overflowing accretion stream in Hellier's (1996, his Fig. 10; also see Hellier 1999, his Fig. 3) schematic diagram of the tomogram expected to result from his stream overflow model for the SW Sex stars. However, as mentioned in § 4, the low-velocity absorption region in our tomograms of V442 Oph, and, to varying degrees, those of the other low-inclination SW Sex stars, is displaced from its predicted location in Hellier's schematic tomogram (where it is attributed to the overflowing stream itself).

6. DISCUSSION

6.1. Half-Orbit Tomography

The tomogram of He I λ6678 in LS Peg (Taylor et al. 1999, their Fig. 10) displays an emission region in the $(+V_x, +V_y)$ quadrant similar to that of He I λ4471 in V442 Oph. The simplest explanation would be the actual presence of an enhanced emission region along the $\phi \approx 0.2$ line of sight through the system. Hirose, Osaki, & Mineshige (1991) and Meglicki, Wickramasinghe, & Bicknell (1993) found that their simulations of CV accretion disks developed regions of enhanced thickness at phases of $\approx 0.2, 0.5,$ 0.8. However, this behavior is expected primarily for low-mass ratio systems, q $(=M_2/M_{wd}) \lesssim 0.15$, whereas CVs with $P_{orb} \approx 0.10$–0.15 days are expected to have higher mass ratios, $q \approx 0.3$–0.5 (Smith & Dhillon 1998). Yet, Rodríguez-Gil et al. (1999) note the presence of a puzzling posteclipse (orbital phase ≈ 0.2) hump in their light curves of the SW Sex star WX Ari, which suggests the possible presence of material of higher luminosity that is visible along this line of sight. Unfortunately, the available light curves of V442 Oph do not reveal a similar such feature. V795 Her has Balmer and He II tomograms quite similar to those of V442 Oph and LS Peg, but its He I λ6678 tomogram is *also* similar in appearance to the Balmer lines (Casares et al. 1996, their Fig. 10), while its He I λ4471 tomogram (which shows a prominent *emission* region at the velocity origin) is different from both the Balmer lines and He I in V442 Oph. Taylor et al. (1999) attribute their odd He I tomogram of LS Peg to violation of the visibility

assumption of Doppler tomography (as we discussed in § 4). We tend to agree with that assessment for V442 Oph also, given that its He I lines are severely affected by the transient absorption event.

We have constructed "half-orbit tomograms" of V442 Oph (similar to those utilized by Hoard et al. 1998 in studying the SW Sex star UU Aquarii) by using only the spectra in the orbital phase range 0.6–0.1; i.e., those that are unaffected by the transient absorption event. These tomograms are shown in Figure 9 in the same format as Figure 4. The He II tomogram is reassuringly unchanged compared to Figure 4—as expected since the He II emission never manifests the absorption feature. The Balmer line tomograms in Figure 9 show much less pronounced low-velocity absorption than in Figure 4, but the former are otherwise indistinguishable from the latter. The He I $\lambda4471$ tomogram in Figure 9 is quite messy (owing to the relative weakness of this line and the reduced number of spectra used in creating the tomogram), but, as with the Balmer lines, the low-velocity absorption is much less prominent. The unusual emission region in the $(+V_x, +V_y)$ quadrant is still present. We inspected the forward-projections of both the full- and half-orbit He I tomograms: they produce trailed spectra in which the bright, redshifted emission region at $\phi \approx 0.6$–0.7 (see Fig. 8) has been "reflected" as a blueshifted region of comparable brightness at $\phi \approx 0.1$–0.2. The latter region is

not present in the original trailed spectrum; hence, it is an artifact of the tomogram creation process caused by the nonuniform visibility of emitting regions in the disk (e.g., see discussion concerning the limitations of Doppler tomography in § 2.4 of Kaitchuck et al. 1994).

6.2. V442 Oph in the Context of the SW Sex Stars

The identification of V442 Oph as an SW Sex star is now quite firm. This CV compares favorably with many of the distinguishing characteristics of the SW Sex stars, including orbital phase–dependent behavior of its emission lines and appearance of its Doppler tomograms. The admission of V442 Oph to this group now brings the total number of bona fide low-inclination (i.e., noneclipsing) SW Sex stars to three,[4] which offers some hope of being able to distinguish between the characteristics of eclipsing and noneclipsing SW Sex stars. For example, as discussed in § 5.2, V442 Oph, like the other low-inclination SW Sex stars, displays a very high velocity emission component in its Balmer lines. Martínez-Pais et al. (1999) have suggested that this component is present in the high-inclination SW Sex stars as a broad line wing that "detaches" from the line core in the

[4] A fourth system, BP Lyncis, is a borderline case displaying an eclipse of the bright spot only and some unusual spectroscopic properties compared to the "normal" SW Sex stars (Hoard & Szkody 1996).
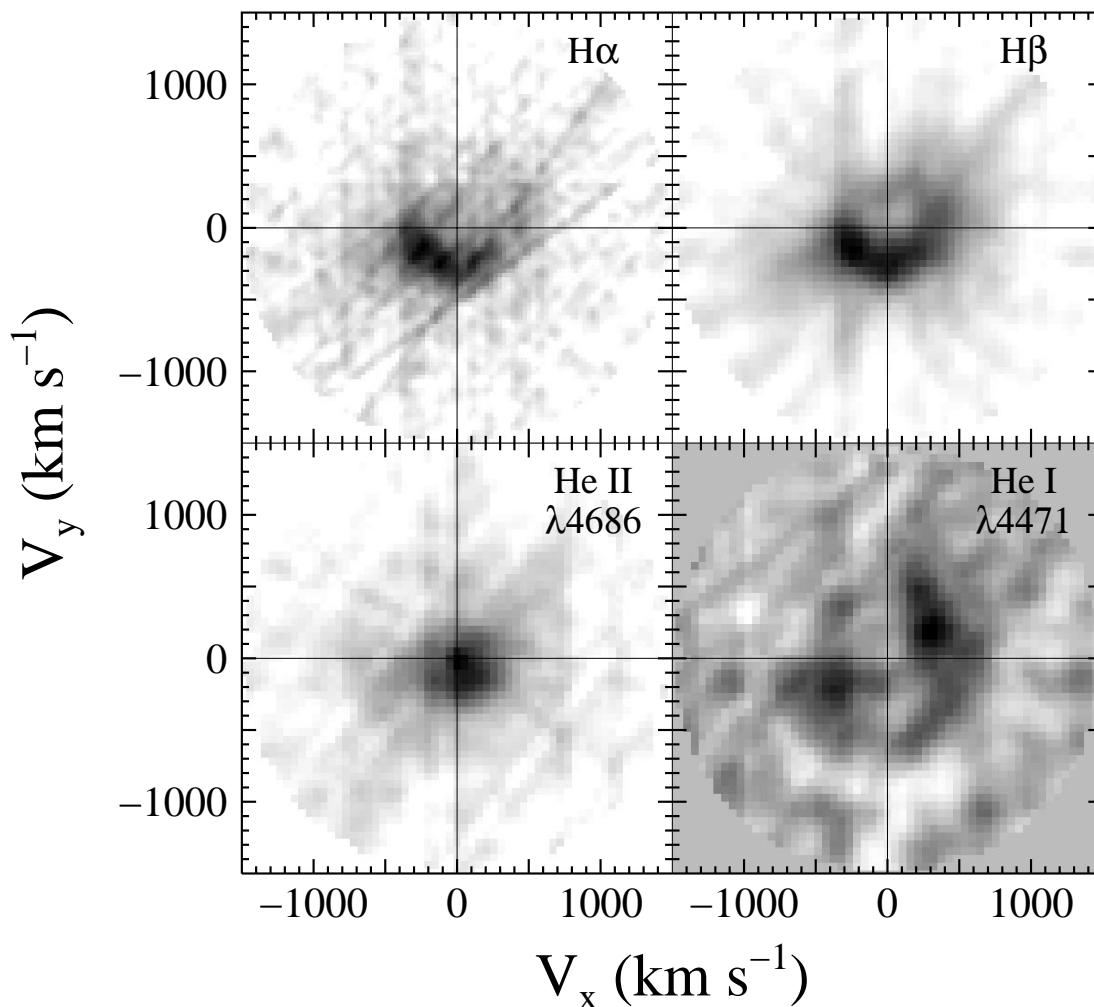

FIG. 9.—As in Fig. 4, but the tomograms have been constructed using only the "unabsorbed" spectra in the orbital phase range 0.6–0.1

low-inclination systems. This requires the emission source to have some component of motion in the vertical plane relative to the disk, possibly in the infall of the overflowing accretion stream to its secondary impact site in the inner disk (although Martínez-Pais et al. have described some apparent discrepancies between the observed and expected velocity maxima for this scenario). We note here that the label "low-inclination" is somewhat misleading since these three CVs could still have inclinations as high as 65°–75° without displaying observable eclipses. Current estimates of their inclinations based on observational properties are $i = 56°$ for V795 Her (Casares et al. 1996), $i < 60°$ (or a model-dependent value of $i = 30°$) for LS Peg (Taylor et al. 1999), and $i \sim 67°$ for V442 Oph (Ritter & Kolb 1998 and references therein).

6.2.1. Accretion Stream Overflow

There are, by now, a large number of competing models, often conflicting and seldom cooperating, that have been proposed to explain the observational characteristics of the SW Sex stars. These models have variously included such mechanisms as bipolar winds (Honeycutt, Schlegel, & Kaitchuck 1986), strong (Williams 1989) or weak (Casares et al. 1996) WD magnetic fields, accretion stream overflow (Hellier & Robinson 1994), nonaxisymmetric vertical structure in the disk (Hoard 1998), magnetic propellors (Horne 1999), and so on. None has been completely satisfactory. These numerous models are extensively reviewed, compared, and critiqued elsewhere (e.g., Warner 1995; Hoard 1998; Hellier 1999). Instead of repeating this procedure here, we focus on one mechanism that appears to be overwhelmingly likely to be operating in some fashion in the SW Sex stars: accretion stream overflow. This phenomenon is predicted by analytical and numerical simulations of accretion stream–disk interaction (e.g., Hessman 1999; Armitage & Livio 1996, 1998) and its presence in other types of interacting binary stars is also suggested by observations (e.g., intermediate polars, Hellier 1993; supersoft X-ray sources, Schandl, Meyer-Hofmeister, & Meyer 1997; X-ray binaries, Frank, King, & Lasota 1987).

Two models prominently feature the accretion stream overflow mechanism. (1) Hellier & Robinson (1994) proposed an overflowing stream with a reimpact site in the inner disk, in concert with a flared disk (Hellier 1998) and, most recently, a disk wind (Hellier 1999). The phase-dependent absorption is produced by the overflowing stream absorbing underlying disk emission, operating in conjunction with the flared disk, which restricts visibility of the absorption to specific orbital phases. (2) Hoard (1998; Hoard et al. 1998) has championed a similar model in which, depending on small differences in mass transfer rate and disk density, the stream either overflows its initial impact site (and continues over the disk surface to reimpact in the inner disk) or impacts explosively with the disk edge (causing material to flow around the outer edge of the disk). The phase-dependent absorption events are caused by obscuration of disk emission by nonaxisymmetric vertical structure built up at either the stream reimpact site in the inner disk (at $\phi \approx 0.5$) or at the initial stream impact site on the disk edge (at $\phi \approx 0.8$), respectively.

A drawback of both models is that the number of free parameters available is large enough (and growing!) that their explanatory and predictive powers are seriously diluted. Additionally, the presence of substantial phase-

dependent absorption events in V442 Oph and the other two low-inclination SW Sex stars, which should be least affected by Hellier's flared disk or Hoard's vertical structure (both of which require viewing the system at high inclination to be most effective), raises an additional issue that must be resolved (although hopefully not by the addition of more free parameters to the models!). Both Taylor et al. (1999) and Martínez-Pais et al. (1999) have pointed out, in regard to LS Peg, that Hellier's flared disk cannot account for the phase-dependent absorption in low-inclination systems. We will not belabor that point further here. Taylor et al. (1999) also briefly mention the possibility of utilizing the simulation results of Armitage & Livio (1996, 1998) to circumvent this problem in the low-inclination SW Sex stars. This idea was explored more fully by Hoard (1998) and Hoard et al. (1998) in developing model (2) described
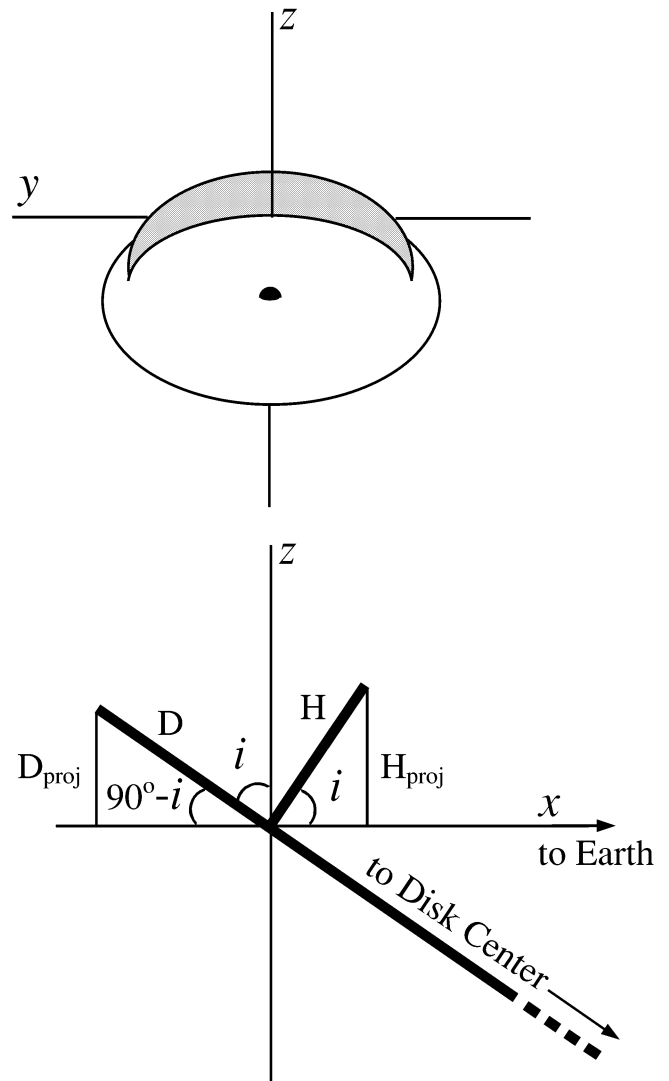

FIG. 10.—*Upper sketch*: An accretion disk with a ridgeline (in gray) positioned at an inclination of $i < 90°$ and orbital phase of 0.25, as viewed from Earth. The (y, z) plane is the plane of the sky, and the secondary star and accretion stream would be located to the right; the white dwarf is shown in black at the center of the disk. *Lower sketch*: A close-up of the disk edge and ridge line, rotated 90° relative to the upper sketch. The x-axis points in the direction of the line of sight to Earth, and the y-axis (not shown) points out of the page. Note that neither sketch is drawn to scale.

above, and we refer the reader to the more detailed descriptions available in those references to supplement the summary given here.

The two main emission regions in the half-orbit tomograms of the Balmer lines in V442 Oph are an approximately circular distribution of relatively weak, diffuse emission, and an intense arc of emission in the $(-V_x, -V_y)$ quadrant. The former region can be caused by emission from material extending above the surface of the disk, possibly in the form of a wind from the disk powered by the disk radiation pressure or a "corona" of material flung up during the initial impact of the stream with the disk edge. The latter region can be caused by hot material flowing "downstream" around the outer edge of the disk from the initial stream impact site. This does not preclude the presence of stream overflow; in fact, stream overflow that builds up a vertically and azimuthally extended "ridgeline" of material directly interior to the disk edge can then account for the phase-dependent absorption. When our line of sight includes the material flowing down the disk edge, then we see the line emission from the hot gas on the disk edge. Along lines of sight from the opposite side of the disk, our view of the hot material on the far disk edge is obscured by the ridgeline. Unlike the flared disk model, this mechanism can operate even at fairly low inclination. The emitting and absorbing regions are immediately adjacent, so it does not require a prohibitively large thickening of the disk to obscure the emitting gas at the disk edge.

A simple geometrical calculation, which is illustrated in Figure 10, can demonstrate this scenario: we determine, for a given system inclination i, the projected height of a vertical structure (the ridgeline) near the edge of the disk that is tall enough to obscure the remainder of the disk outside it when viewed from the opposite side of the disk. In this case, the projected height of the ridgeline above the point where it emerges from the disk is given by

$$H_{\mathrm{proj}} = H \sin i \, ,$$

where H is the true vertical height of the ridgeline above the disk surface. The projected vertical extension of the remainder of the disk outside of the ridgeline, as viewed from the opposite side of the disk, is

$$D_{\mathrm{proj}} = D \sin (90° - i) \, ,$$

where D is the distance from the edge of the disk inward to the ridgeline. So, we require that $H_{\mathrm{proj}} \gtrsim D_{\mathrm{proj}}$, or

$$H \gtrsim D \, \frac{\sin (90° - i)}{\sin i} \, .$$

For example, if $i = 50°$, then the height of the vertical structure above the disk surface need only be 84% of the distance

from the edge of the disk in order to obscure the outer disk when viewed from the opposite side of the disk; i.e., if the ridgeline is located at $r = 0.9 R_{\mathrm{disk}}$, where R_{disk} is the radius of the accretion disk, then it only needs to be $0.084 R_{\mathrm{disk}}$ tall in order to produce the phase-dependent absorption for all inclinations of $i \gtrsim 50°$. We note that this is the height required to obscure the outer edge of the disk completely, but in principle only a fraction of the outer disk must be obscured by the ridgeline (because the emission does not completely vanish during the absorption-affected orbital phases), so the estimate of the height of the ridgeline is most likely an upper limit.

7. CONCLUSIONS

Our spectroscopic observations of the cataclysmic variable V442 Oph, which span 4 yr from 1995 to 1999, have yielded several interesting results about this star:

1. We have broken the 1 day orbital period alias for this CV. With $P_{\mathrm{orb}} = 0.1243$ days, V442 Oph is located at the long period end of the CV period gap.

2. Its spectroscopic behavior and Doppler tomogram appearance confirm V442 Oph as a low-inclination SW Sex star.

3. Like the other two low-inclination SW Sex stars (V795 Her and LS Peg), V442 Oph shows a very high velocity emission component in its Balmer emission lines. This component maps to a location in the Doppler tomograms consistent with the reimpact in the inner disk of an overflowing accretion stream.

4. The behavior of V442 Oph is consistent with the presence of accretion stream overflow. In addition to the high-velocity emission component, the main emission region of the Doppler tomograms suggests accreting material splashes up at the initial stream impact site and flows over the disk surface and around the disk edge.

5. Nonaxisymmetric vertical structure can still account for the phase-dependent absorption in this (and other) low-inclination SW Sex stars, while a flared disk cannot. However, the exact nature of the mechanism producing the phase-dependent absorption in the SW Sex stars remains largely unknown.

REFERENCES

Armitage, P. J., & Livio, M. 1996, ApJ, 470, 1024
———. 1998, ApJ, 493, 898
Beuermann, K., Thorstensen, J. R., Schwope, A. D., Ringwald, F. A., & Sahin, H. 1992, A&A, 256, 442
Casares, J., Martínez-Pais, I. G., Marsh, T. R., Charles, P. A., & Lázaro, C. 1996, MNRAS, 278, 219
Chen, J.-S., Jiang, Z.-J., Li, Y., Liu, X.-W., & Feng, X.-C. 1993, Acta Astrophys. Sinica, 13, 225
Dickinson, R. J., Prinja, R. K., Rosen, S. R., King, A. R., Hellier, C., & Horne, K. 1997, MNRAS, 286, 44
Frank, J., King, A. R., & Lasota, J.-P. 1987, A&A, 178, 137
Gillespie, B., Loewenstein, R. F., & York, D. 1995, in ASP Conf. Ser. 87, New Observing Modes for the Next Century, ed. T. Boroson, J. Davies, & I. Robson (San Francisco: ASP), 97

Hellier, C. 1993, PASP, 105, 966
———. 1996, ApJ, 471, 949
———. 1998, PASP, 110, 420
———. 1999, New Astron. Rev., in press
Hellier, C., Ringwald, F. A., & Robinson, E. L. 1994, A&A, 289, 148
Hellier, C., & Robinson, E. L. 1994, ApJ, 431, L107
Hessman, F. V. 1999, ApJ, 510, 867
Hirose, M., Osaki, Y., & Mineshige, S. 1991, PASJ, 43, 809
Hoard, D. W. 1998, Ph.D. thesis, Univ. of Washington
Hoard, D. W., Still, M. D., Szkody, P., Smith, R. C., & Buckley, D. A. H. 1998, MNRAS, 294, 689
Hoard, D. W., & Szkody, P. 1996, ApJ, 470, 1052
———. 1997, ApJ, 481, 433
———. 1999, New Astron. Rev., in press

Honeycutt, R. K., Schlegel, E. M., & Kaitchuck, R. H. 1986, ApJ, 302, 388
Horne, K. 1991, in Fundamental Properties of Cataclysmic Variable Stars: Proc. of the 12th North American Workshop on Cataclysmic Variables and Low-Mass X-Ray Binaries, ed. A. W. Shafter (San Diego: San Diego State Univ.), 23
————. 1999, New Astron. Rev., in press
Kaitchuck, R. H., Schlegel, E. M., Honeycutt, R. K., Horne, K., Marsh, T. R., White, J. C., II, & Mansperger, C. S. 1994, ApJS, 93, 519
Martínez-Pais, I. G., Rodríguez-Gil, P., & Casares, J. 1999, MNRAS, 305, 661
Massey, P., Strobel, K., Barnes, J. V., & Anderson, E. 1988, ApJ, 328, 315
Meglicki, Z., Wickramasinghe, D., & Bicknell, G. V. 1993, MNRAS, 264, 691
Ritter, H., & Kolb, U. 1998, A&AS, 129, 83
Rodríguez-Gil, P., Casares, J., Dhillon, V. S., & Martínez-Pais, I. G. 1999, A&A, in press (astro-ph/9911303)
Schandl, S., Meyer-Hofmeister, E., & Meyer, F. 1997, A&A, 318, 73
Schneider, D. P., & Young, P. 1980, ApJ, 238, 946
Shafter, A. W. 1992, ApJ, 394, 268

Smith, D. A., & Dhillon, V. S. 1998, MNRAS, 301, 767
Szkody, P. 1991, in Fundamental Properties of Cataclysmic Variable Stars: Proc. of the 12th North American Workshop on Cataclysmic Variables and Low Mass X-Ray Binaries), ed. A. Shafter (San Diego: San Diego State Univ.), 56
Szkody, P., & Piché, F. 1990, ApJ, 361, 235
Szkody, P., & Shafter, A. W. 1983, PASP, 95, 509
Szkody, P., & Wade, R. A. 1980, PASP, 92, 806
Taylor, C. J., Thorstensen, J. R., & Patterson, J. 1999, PASP, 111, 184
Thorstensen, J. R., & Freed, I. B. 1985, AJ, 90, 2082
Thorstensen, J. R., Patterson, J., Shambrook, A., & Thomas, G. 1996, PASP, 108, 73
Thorstensen, J. R., Ringwald, F. A., Wade, R. A., Schmidt, G. D., & Norsworthy, J. E. 1991, AJ, 102, 272
Thorstensen, J. R., Taylor, C. J., & Kemp, J. 1998, PASP, 110, 1405
Warner, B. 1995, Cataclysmic Variable Stars (Cambridge: Cambridge Univ. Press)
Williams, R. E. 1989, AJ, 97, 1752